◆ CLINICAL INVESTIGATION ◆

Multislice CT Angiography in the Follow-up of Fenestrated Endovascular Grafts: Effect of Slice Thickness on 2D and 3D Visualization of the Fenestration Stents

Zhonghua Sun, PhD[1]; Yvonne B. Allen, RN[2]; Bibombe P. Mwipatayi, MMed (Surg), FCS(SA), FRACS[3]; David E. Hartley, FIR[2]; and Michael M.D. Lawrence-Brown, FRACS[4]

[1]Discipline of Medical Imaging, Department of Imaging and Applied Physics. [2]Cook R&D, Perth, Western Australia. [3]Department of Vascular Surgery, Royal Perth Hospital, Perth, Western Australia. [4]School of Public Health, Curtin University of Technology, Perth, Western Australia.

Purpose: To investigate the effect of multislice computed tomography (CT) protocols on the visualization of target vessel stents in patients with abdominal aortic aneurysm (AAA) treated with fenestrated endovascular grafts.

Methods: Twenty-one patients (19 men; mean age 75 years, range 63–86) undergoing fenestrated endovascular repair of AAA were retrospectively studied. Multislice CT angiography was performed with several protocols, and the section thicknesses used in each were compared to identify any relationship between slice thickness and target vessel stents visualized on 2-dimensional (2D) axial, multiplanar reformatted (MPR), and 3-dimensional (3D) virtual intravascular endoscopy (VIE) images. Image quality was assessed based on the degree of artifacts and their effect on the ability to visualize the configuration, intra-aortic location, and intraluminal appearance of the target vessel stents and measure their protrusion into the aortic lumen.

Results: There were 7 different multislice CT scanning protocols employed in the 21 patients (25 datasets, with 2 sets of follow-up images in 4 patients). The slice thicknesses and numbers (n) of studies included were 0.5 (n=3), 0.625 (n=6), 1.0 (n=1), 1.25 (n=9), 2.5 (n=3), 3.0 (n=1), and 5.0 mm (n=2). Of these CT protocols, images (especially 2D/3D reconstructions) acquired at 2.5, 3.0, and 5.0 mm were significantly compromised by interference from artifacts. Images acquired with a slice thickness of 1.0 or 1.25 mm were scored equal to or lower than those acquired with a submillimeter section thickness (0.5 or 0.625 mm), with minor degrees of artifacts resulting in acceptable image quality.

Conclusion: Visualization of the target vessel stents depends on the appropriate selection of multislice CT scanning protocols. Our results showed that studies performed with a slice thickness of 1.0 or 1.25 mm produced similar image quality to those with a thickness of 0.5 or 0.625 mm. Submillimeter slices are not recommended in imaging patients treated with fenestrated stent-grafts, as they did not add additional information to the visualization.

J Endovasc Ther 2008;15:417–426

Yvonne Allen is an employee of Cook R&D Australia. David Hartley is a consultant to Cook R&D Australia and receives royalties from the Zenith endograft. Michael Lawrence-Brown is a consultant to the Cook Group companies and receives royalties from the Zenith endograft. The other authors have no commercial, proprietary, or financial interest in any products or companies described in this article.

Address for correspondence and reprints: Dr. Zhonghua Sun, Discipline of Medical Imaging, Department of Imaging and Applied Physics, Curtin University of Technology, GPO Box U1987, Perth, Western Australia 6845. E-mail: *z.sun@curtin.edu.au*

Key words: endovascular aneurysm repair, surveillance, multislice computed tomography, slice thickness, fenestrated stent-graft, image quality, visualization

Endovascular repair of abdominal aortic aneurysm (AAA) using fenestrated stent-grafts evolved to treat patients with short aneurysm necks.[1–3] The principle of fenestration is to preserve blood flow to renal or visceral vessels and enhance stability by inserting bare or covered stents into side branches to produce a durable relationship between the graft fenestration and the branch artery ostium. With stents in position, a balloon is typically inflated to deploy the stent within the renal or other visceral arteries.[2,3] At this point, the stents are normally flared with a balloon to secure the fenestration to the side branch ostium, so there exists a risk of distorting or deforming the implanted stents. Thus, accurate evaluation of the appearance of target vessel stents, especially the intra-aortic portion, is of paramount importance for endovascular specialists to assess the treatment outcomes of the procedure.

Imaging techniques play an important role in the detection of any abnormalities associated with fenestrated endovascular repair. Helical computed tomographic (CT) angiography is the routine technique used to assess the patency of the fenestration vessels and target vessel stents in relation to the arterial branches.[4] In recent years, the diagnostic value of CT angiography in fenestrated stent-grafting has been significantly augmented with the development of the multislice CT imaging technique.[5] In addition to conventional 2-dimensional (2D) axial images, a series of 2D or 3-dimensional (3D) reconstructions are commonly generated to enhance the understanding of stent-grafts in relation to the aortic branches. These reconstructions include multiplanar reformation (MPR), maximum intensity projection, volume rendering, and virtual intravascular endoscopy (VIE). These reconstructions provide valuable information used in the evaluation of traditional infrarenally or suprarenally affixed stent-grafts.[6–8]

One of the main limitations of CT imaging in the evaluation of fenestrated stent-grafts is overestimation of the stent wire thickness, which is determined mainly by the slice thickness. With the current 64-slice CT scanner, a voxel size of $0.4\times0.4\times0.4$ mm can be achieved, so a thin-slice thickness (submillimeter) is commonly applied to scan patients, presumably to enhance image quality with higher resolution.[9] However, this is not always the case; it is well known that thin slice thickness results in high image noise or a low signal-to-noise ratio.[10,11] Moreover, radiation dose is another important issue to be considered when selecting the CT scanning protocol, especially for the protocols with thinner slice thicknesses.[12,13] These issues have not drawn endovascular specialists' attention in the follow-up of patients using multislice CT technique, so the aim of this study was to investigate the effect of multislice scanning protocols, mainly slice thickness, on the visualization of target vessel stents based on 2D axial, MPR, and VIE images in a group of AAA patients treated with fenestrated stent-grafts.

METHODS

Patient Data Selection

Twenty-one patients (19 men; mean age 75 years, range 63–86) with AAA treated by implantation of a fenestrated endovascular graft were retrospectively reviewed for this study. Sixty-four side branches were targeted for fenestrations of 4 types: scalloped (minimum 10-mm width and a height range of 6 to 12 mm), double-width scalloped (20×20 mm), large (8×8 or 10×10 mm), and small (6×6 or 6×8 mm). Scalloped fenestrations were placed in 17 aortic branches [8 celiac axis and 9 superior mesenteric artery (SMA)], large fenestrations were placed in 8 aortic branches (1 celiac axis and 7 SMAs), and small fenestrations were placed in 39 arterial branches (19 right renal arteries and 20 left renal arteries).

In this cohort, 25 multislice CT datasets were identified (including 2 sets of follow-up images in 4 patients) in the analysis. As

TABLE 1
Assessment of Image Quality Corresponding With Different Multislice CT Scanning Protocols

Slice Thickness, mm	Visualization of Target Vessel Stents*		
	2D Axial	MPR	VIE
0.5 (n=3)	1.3	1.3	1.3
0.625 (n=6)	1.3	1.3	1.3
1.0 (n=1)	1	1	1
1.25 (n=9)	1	1.2	1.4
2.5 (n=3)	2.3	2.7	2.7
3.0 (n=1)	2	2	3
5.0 (n=2)	2	3.5	3.5

2D: 2-dimensional, MPR: multiplanar reformation, VIE: virtual intravascular endoscopy.
* Average score based on 1: target vessel stents are clearly visualized with minor or no artifacts, 2: target vessel stents are visualized with moderate artifacts, 3: target vessel stents are visualized with severe artifacts, and 4: target vessel stents cannot be visualized.

patients were referred from different vascular centers in Western Australia, the CT scans were performed with different equipment [24 scans were done on a Light-Speed scanner (GE Medical Systems, Milwaukee, WI, USA) and 1 on an Aquilion scanner (Toshiba Medical Systems, Kingsbury, UK)]. The slice thickness used in our study group ranged from 0.5 to 5.0 mm. Table 1 lists the scanning protocols identified in the 25 CT scans.

Data Postprocessing and Image Reconstruction

Original DICOM (Digital Imaging and Communication in Medicine) data were transferred to a workstation equipped with Analyze V 7.0 (AnalyzeDirect, Inc., Lexana, KS, USA) for generation of 2D and 3D reconstructed images. First, the 2D axial images were reviewed in each patient, followed by the reconstruction of MPR images showing the target vessel stents, mainly in the renal arteries. The Analyze software allowed the user to generate multiplanar views in any given plane and to view the images in both fixed and cine imaging formats. In addition, VIE images were included to visualize the intraluminal appearance of target vessel stents. The methodology used to generate VIE has been described elsewhere.[6,7]

Image Assessment

For visualization of the target vessel stents, the focus was on both the intra-aortic portion and the extra-aortic stents based on 2D axial and MPR images. With VIE visualization, the aim was to demonstrate the intraluminal appearance of target vessel stents with regard to the type of fenestration employed in each patient. Characterization of the intraluminal stent appearance on VIE images has been reported previously[8] and was applied in this correlation of the slice thickness with corresponding VIE images to provide unique intraluminal views of fenestration stents that can assist endovascular specialists in detecting any postprocedural abnormalities or complications. The intraluminal stent appearance was classified into 4 types: I referred to a circular appearance, II was a circular appearance with a flaring effect at the inferior portion of the stent wires, III referred to an elliptical appearance with flaring effect at the inferior portion of the stent wires, and IV indicated no stent wires observed, only markers. Most commonly, type IV referred to scalloped fenestrations because normally there is no stent inserted into this type of fenestration.

The presence of windmill or blooming artifacts caused by the stent wires was analyzed in each visualization mode. A 4-point scoring scale was used according to our previous experience in 3D imaging of endovascular aneurysm repair to assess the quality of 2D and 3D images.[10,14] Score 1 was target vessel stents clearly visualized with minor or no artifacts, score 2 referred to target vessel stents visualized with moderate artifacts, score 3 was stent visualization with severe artifacts, and score 4 indicated no visualization of the target vessel stents. Each imaging modality was scored with regard to the appearance (either intraluminal or extraluminal) of the target vessel stents. Each patient's data were scored individually for the 3 visualization tools, and an average score was calculated for the number of cases using each scanning protocol. Images scored with 1

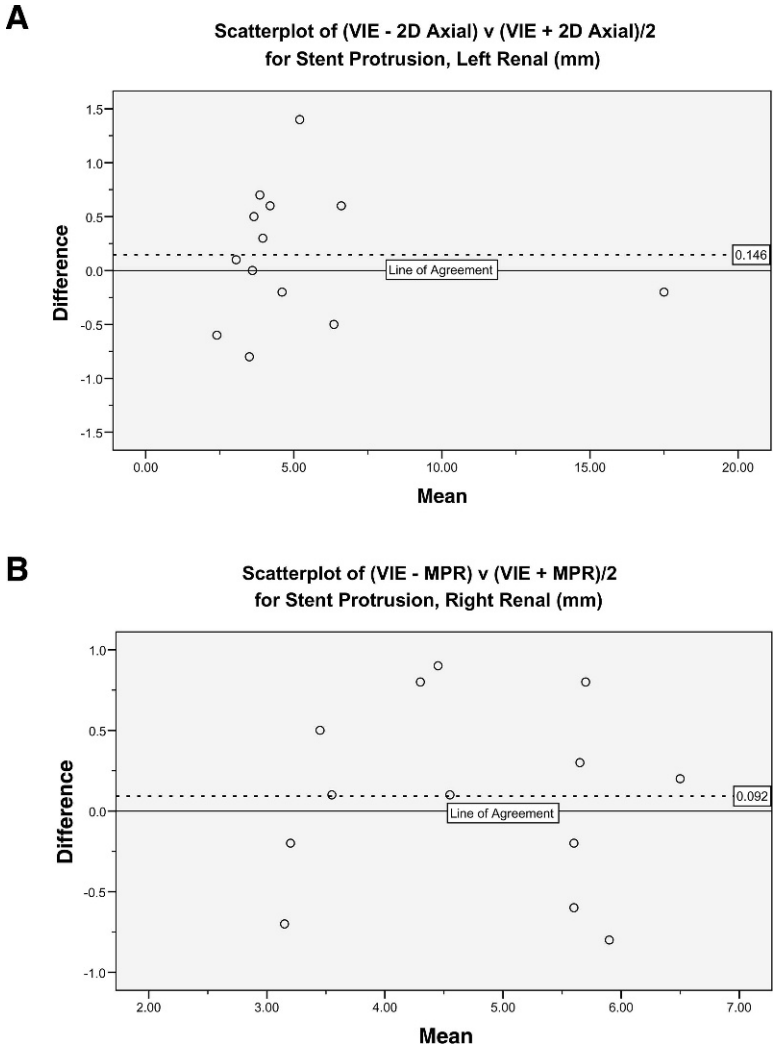

Figure 1 ◆ Examples of scatterplots comparing VIE with axial scans in the left renal artery (**A**) and VIE with MPR in the right renal artery (**B**) for measurement of stent protrusion length. The mean difference between these measurements was not significantly different from zero, nor was the correlation coefficient.

or 2 were considered acceptable for diagnostic purposes, while images with a score of 3 or 4 were deemed to be significantly affected by the artifacts and not acceptable for diagnosis.

Measurement of Stent Protrusion Into the Abdominal Aorta

In addition to 2D axial images, MPR and VIE images were used to measure the length of stents protruding into the abdominal aorta after fenestrated endovascular repair. The measurements were performed by one of the authors (Z.S.) with more than 9 years' experience in 3D CT imaging of aortic stent-grafts. The length of stent protrusion was measured 3 times at each location, and the mean values were used to avoid intraobserver disagreement.

Statistical Analysis

The differences in measurements of stent protrusion between VIE and MPR and VIE and axial images were tested using linear regression analysis and displayed in scatterplots as differences versus means. If there was no

TABLE 2
Stent Protrusion Measured With 2D Axial, MPR, and VIE Images

Case	Slice Thickness, mm	Length of Stent Protrusion Measured With 2D Axial/MPR/VIE, mm			
		Celiac Axis	SMA	RRA	LRA
1	0.5	—	—	3.7/3.1/3.2	3.9/3.4/3.6
2	0.5	—	—	3.7/3.1/3.2	3.9/3.4/3.6
3	0.5	—	—	—	5.9/4.9/5.5
4	0.625	4.4/4.4/5.3	3.4/4.4/3.8	5.5/4.9/5.7	6.9/6.3/6.4
5	0.625	—	5.4/5.6/5.8	5.3/5.2/5.9	17.3/17.3/17.8
6	0.625	—	—	5.9/4.0/4.6	4.0/4.0/4.4
7	0.625	—	8.7/8.5/8.5	3.6/3.2/3.5	3.6/3.6/3.6
8	0.625	—	—	—	5.8/5.3/5.2
9	0.625	—	—	4.8/4.6/5.1	4.6/4.5/4.6
10	1.0	—	—	4.8/5.1/5.3	4.8/4.7/4.6
11	1.25	—	—	3.3/3.5/3.9	2.5/2.4/3.0
12	1.25	—	5.7/4.5/4.4	6.6/6.3/6.4	4.2/3.5/3.6
13	1.25	—	4.8/4.2/3.9	5.5/5.9/6.3	6.1/6.6/6.0
14	1.25	—	4.0/3.9/4.2	4.7/4.4//3.9	4.5/3.9/4.0
15	1.25	—	—	3.1/3.1/3.3	3.1/3.0/3.3
16	1.25	—	3.3/4.0/4.6	4.9/4.0/4.0	—
17	1.25	—	—	5.6/5.0/5.0	2.5/2.0/2.7
18	1.25	—	—	4.1/3.8/4.6	5.3/4.9/4.6
19	1.25	—	—	4.9/4.0/4.1	2.4/2.4/2.9
20	2.5	—	—	NA	NA
21	2.5	—	—	4.0/4.1/4.5	2.3/2.4/2.8
22	2.5	—	—	4.6/4.5/4.5	2.1/2.7/2.7
23	3.0	—	8.8/8.3/7.8	4.1/2.6/2.9	3.2/2.8/3.2
24	5.0	—	—	3.6/NA/NA	NA/NA/NA
25	5.0	—	—	4.0/NA/NA	4.4/NA/NA

2D: 2-dimensional, MPR: multiplanar reformation, VIE: virtual intravascular endoscopy, SMA: superior mesenteric artery, RRA: right renal artery, LRA: left renal artery, NA: not available.

trend in the bias (difference), then the scatterplot appears random (Fig 1). If there is a trend, it appears as a statistically significant correlation. $P<0.05$ indicated a statistically significant difference. Analyses were performed using SPSS software (version 14.0; SPSS, Chicago, IL, USA).

RESULTS

Our results showed that images acquired with a slice thickness of >2.5 mm received scores higher than those acquired with a slice thickness <2.5 mm, mainly due to the presence of moderate or severe artifacts on protocols with thicker slices, especially the 5.0-mm slices, which received the highest score. Images acquired with thinner slices, such as 0.5, 0.625, 1.0, and 1.25 mm, were scored similarly for all 3 imaging modalities.

Table 2 presents the length of stent protrusion into the abdominal aortas measured with the 3 visualization modalities. Most of the stents protruded between 3.0 and 7.0 mm, while in 2 exceptional cases (1 SMA and 1 left renal fenestration), the length exceeded 8.0 mm. Our results showed there was no statistically significant difference between 2D axial and MPR, MPR and VIE, or 2D axial and VIE visualizations in the measurement of stent protrusion ($p>0.05$). For images acquired with thicker slices (>2.5 mm), stent protrusion could not be measured in 1 of the 3 cases scanned at 2.5 mm or in the 2 cases scanned at 5.0 mm. For the images acquired with thinner slices ranging from 0.5 to 1.25 mm, stent length was successfully measured in all cases.

Table 3 provides information about the intraluminal appearance of target vessel stents visualized on VIE images. VIE charac-

TABLE 3
Types of Fenestration Deployed Per Procedure and Intraluminal Appearance of Target Vessel Stents Visualized With VIE

	Type of Fenestration/Intraluminal Appearance of Target vessel Stents			
Cases	Celiac Axis	SMA	RRA	LRA
1	—	—	Small/II	Small/I
2	—	—	Small/I	Small/II
3	—	—	—	Small/I
4	Large/I	Large/I	Small/I	Small/I
5	—	Large/I	Small/I	Small/I
6	—	Scallop/IV	Small/I	Small/I
7	DW Scallop/IV	Large/III	Small/I	Small/II
8	—	—	—	Small/I
9	DW Scallop/IV	Scallop/IV	Small/I	Small/II
10	DW Scallop/IV	Scallop/IV	Small/I	Small/II
11	Scallop/IV	Scallop/IV	Small/II	Small/II
12	DW Scallop/IV	Large/III	Small/I	Small/III
13	DW Scallop/IV	Large/II	Small/II	Small/III
14	DW Scallop/IV	Large/I	Small/II	Small/III
15	—	Scallop/IV	Small/I	Small/II
16	DW Scallop/IV	Large/I	Small/I	—
17	—	DW Scallop/IV	Small/I	Small/II
18	—	Scallop/IV	Small/II	Small/II
19	—	Scallop/IV	Small/I	Small/II
20	—	—	NA	NA
21	—	Scallop/IV	Small/I	Small/II
22	—	Scallop/IV	Small/I	Small/I
23	—	Large/III	Small/I	Small/III
24	—	NA	NA	NA
25	—	NA	NA	NA

SMA: superior mesenteric artery, RRA: right renal artery, LRA: left renal artery, NA: not available, DW: double width, I: circular appearance, II: circular with flaring effect, III: elliptical with flaring effect, and IV: only markers on stents wires are visualized.

terized the stents successfully in most of the thinner slices, while in slices >2.5 mm thick, image quality was significantly compromised due to artifacts. As shown in the Table, 39% of the target vessel stents were demonstrated on VIE as type I (circular), while 26% of the stents were type II (circular with flaring). Only 8% of the stents were type III. All of the scalloped fenestrations (whether standard or double-width) were type IV (27%) because no fenestration stents were placed.

Figures 2 to 4 show a number of 2D axial, MPR, and VIE images, respectively, acquired with variable slice thicknesses. The effect of slice thickness on the 2D axial images is seen in both thinner (0.5 mm) and thicker (2.5 mm) slices, with moderate artifacts. For MPR and VIE images, thinner slices most commonly produced better image quality. Moderate or severe artifacts were present in images acquired with a slice thickness >2.5 mm in both MPR and VIE images, which interferes with the visualization of target vessel stents to a great extent.

DISCUSSION

This study was designed to investigate the effect of multislice CT scanning protocols on the visualization of target vessel stents in AAA patients treated with fenestrated stent-grafts. Thus, research arising from this report is of potential benefit to endovascular specialists in choosing appropriate multislice CT scanning protocols when following patients treated with fenestrated endovascular grafts.

Helical CT angiography has been widely regarded as the preferred imaging modality in both preoperative planning and postoperative surveillance of endovascular stent-

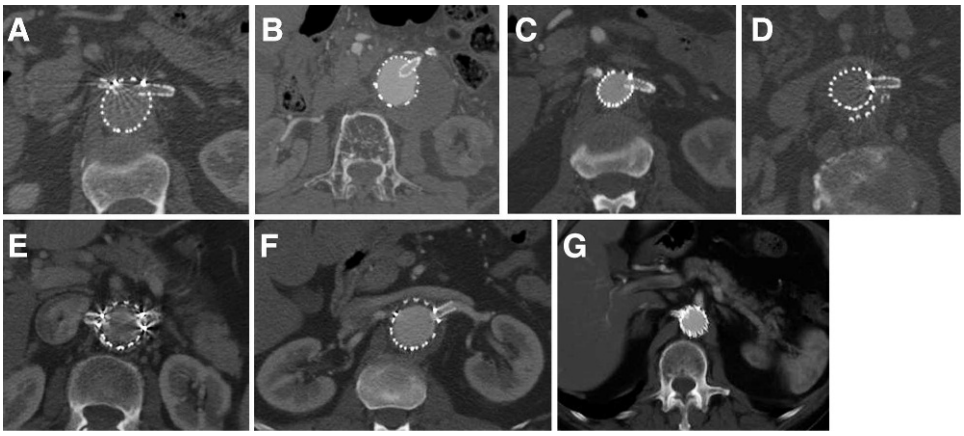

Figure 2 ◆ Axial CT images of the renal stents were acquired with variable slice thicknesses (0.5, 0.625, 1.0, 1.25, 2.5, 3.0, and 5.0 mm, respectively, in **A**–**G**). Visualization of the renal stents was affected with both thin (0.5 mm in **A**) and thick slices (2.5 mm in **E**).

grafts.[15,16] In recent years, the role of helical CT imaging has been greatly enhanced with the development of multislice scanners, which demonstrate superior spatial and temporal resolution over traditional single-slice CT.[5] However, selection of the optimal multislice CT scanning protocol in imaging of fenestrated stent-grafts has not been studied systematically, to the best of our knowledge.

As already known, capturing CT images using thin slices results in higher spatial resolution, which improves detection of tiny structures, such as stent wires. This is especially important for 2D or 3D reconstructions, such as MPR or VIE. As shown in our results, both MPR and VIE visualizations of the fenestration stents were significantly affected when the slice thickness was >2.5 mm. However, the thin slices that are available with multiple CT detectors are also associated with unfavorable effects, such as increased image noise and higher radiation dose. These effects were confirmed by recent studies comparing different multislice CT detectors in cerebral and cardiac imaging,[12,17] which showed increased radiation dose associated with higher resolution CT scanners. In our study, we did not find a significant difference between a very thin slice (0.5 to 0.625 mm) and relatively thin slices (1.0 to 1.25 mm) in the assessment of target vessel stents. Therefore, we recommend a slice

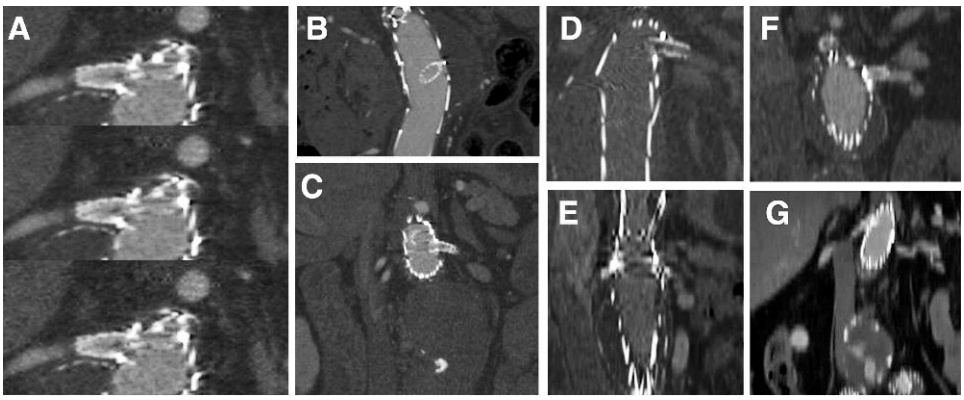

Figure 3 ◆ MPR images of the renal stents were acquired with variable slice thicknesses (0.5, 0.625, 1.0, 1.25, 2.5, 3.0, and 5.0 mm, respectively, in **A**–**G**). When the slice thickness is >2.5 mm, moderate or severe artifacts interfere with visualization of stent wires (**E**–**G**).

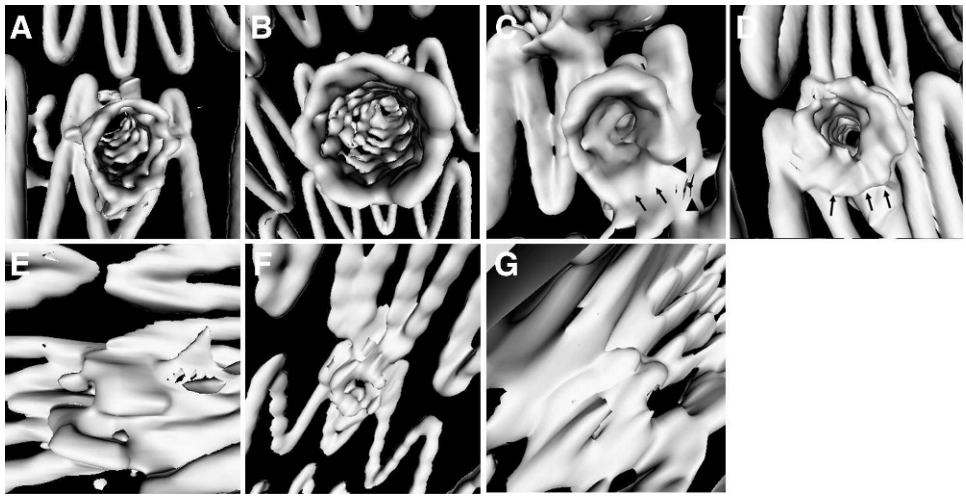

Figure 4 ◆ VIE images looking at the renal stents intraluminally were acquired with different slice thicknesses (0.5, 0.625, 1.0, 1.25, 2.5, 3.0, and 5.0 mm, respectively, in **A**–**G**). Artifacts significantly interfered with visualization of stent wires when the slice thickness was >2.5 mm (**E**–**G**). Arrows in **C** and **D** indicate the flaring effect at the lower end of the fenestration stents, while the arrowheads in **C** refer to the artifacts observed during the image processing.

thickness of 1.0 to 1.25 mm as an appropriate multislice CT protocol in the follow-up of patients with fenestrated stent-grafts; this resolution achieves acceptable image quality while avoiding extra radiation exposure to patients by using submillimeter slice thicknesses.

Most commonly, clinicians have the general impression that thin slices result in better image quality without considering the associated higher radiation dose, which we corroborated to some extent because 36% of the multislice CT scans was performed with a submillimeter slice thickness (0.5 to 0.625 mm). As the clinical application of fenestrated stent-grafts goes back 10 years,[18] many patients have been followed for a long period since they underwent treatment. Therefore, we believe that our findings are valuable for increasing endovascular specialists' awareness of choosing the appropriate multislice CT scanning protocols while reducing the radiation doses associated with thinner slice CT scans.

Characterization of the intraluminal appearance of target vessel stents by VIE is valuable because it provides additional information regarding treatment outcomes.[8] As balloon molding is a routine procedure to flare the stents after implantation of a fenestrated device, there is a possibility of distorting or deforming the vessel stents. Conventional 2D or 3D images provide only external views of the vessel stents, while VIE demonstrates the intraluminal appearance of vessel stents as well as measuring the stent protrusion. About one third of the target vessel stents implanted in our patients were found to have flaring effects at the lower end of the stent wires visualized on VIE. The balloon flaring size is always larger than actual diameters of the stents to ensure the dilation and patency of the inserted stents; this easily leads to configuration changes at the lower portion of the stents, as confirmed by VIE in this study. Moreover, our results showed that VIE is as accurate as 2D axial and MPR images in the measurement of stent protrusion, with no significant difference between these methods. Therefore, we believe VIE could be used as a reliable tool to follow patients treated with fenestrated stent-grafts.

The main limitation of VIE visualization of fenestration stents is the overestimated diameter of stent wires, which prevents accurate assessment of stent diameter. Thus, an appropriate CT scanning protocol is essential to ensure acquisition of images with adequate quality. Based on the findings of this

study, a thin slice <1.0 mm is not necessary for visualization of the target vessel stents since a protocol featuring 1.0- or 1.25-mm slices produced images as good as the submillimeter slice protocols. A slice thickness >2.5 mm is not recommended as image quality is compromised due to partial volume effect, which prevents visualization of target vessel stents based on 2D or 3D images.

Limitations

We did not compare the imaging appearance or stent protrusion at different follow-up periods, which is one of the study limitations. Second, the scoring of these images was performed by one observer, which could introduce bias into the assessment of image quality. Two or three observers involved in the assessment are preferred. Finally, we did not measure the radiation dose associated with each CT scanning protocol.

Conclusion

We have demonstrated the effect of slice thickness on the visualization of target vessel stents in terms of appearance and intra-aortic protrusion. Our results showed that acceptable image quality can be acquired with multislice CT scanning protocols using a slice thickness of 1.0 or 1.25 mm without compromising the assessment of fenestration stents in relation to the branch artery ostium. A thin slice (submillimeter), such as 0.5 or 0.625 mm, is not necessary for imaging of fenestrated stent-grafts considering the higher radiation dose associated with the thinner scanning protocols. Further studies based on phantom experiments are required to validate our results.

Acknowledgments: The authors would like to thank Mr. Gil Stevenson for his assistance in the statistical analysis of the results.

REFERENCES

1. Browne TF, Hartley D, Purchas S, et al. A fenestrated covered suprarenal aortic stent. *Eur J Vasc Endovasc Surg*. 1999;18:445–449.
2. Stanley BM, Semmens JB, Lawrence-Brown MM, et al. Fenestration in endovascular grafts for aortic aneurysm repair: new horizons for preserving blood flow in branch vessels. *J Endovasc Ther*. 2001;8:16–24.
3. Anderson JL, Berce M, Hartley D. Endoluminal aortic grafting with renal and superior mesenteric artery incorporation by graft fenestration. *J Endovasc Ther*. 2001;8:3–15.
4. Sun Z, Mwipatayi BP, Semmens JB, et al. Short to midterm outcomes of fenestrated endovascular grafts in the treatment of abdominal aortic aneurysms: a systematic review. *J Endovasc Ther*. 2006;13:747–753.
5. Rubin GD, Shiau MC, Leung AN, et al. Aorta and iliac arteries: single versus multiple detector-row helical CT angiography. *Radiology*. 2000;215:670–676.
6. Sun Z, Winder J, Kelly B, et al. CT virtual intravascular endoscopy of abdominal aortic aneurysms treated with suprarenal endovascular stent grafting. *Abdom Imaging*. 2003;28:580–587.
7. Sun Z, Winder RJ, Kelly BE, et al. Diagnostic value of CT virtual intravascular endoscopy in aortic stent-grafting. *J Endovasc Ther*. 2004;11:13–25.
8. Sun Z, Allen YB, Nadkarni S, et al. CT virtual intravascular endoscopy in the visualization of fenestrated stent-grafts. *J Endovasc Ther*. 2008;15:42–51.
9. Kyriakou Y, Kachelrie BM, Knaup M, Krause JU, Kalender WA. Impact of the z-flying focal spot in resolution and artefact behaviour for a 64-slice spiral CT scanner. *Eur Radiol*. 2006;16:1206–1215.
10. Sun Z, Gallagher E. Multislice CT virtual intravascular endoscopy for abdominal aortic aneurysm stent grafts. *J Vasc Interv Radiol*. 2004;15:961–970.
11. Sun Z, Ferris C. Optimal scanning protocol of multislice CT virtual intravascular endoscopy in pre-aortic stent grafting: in vitro phantom study. *Eur J Radiol*. 2006;58:310–316.
12. Coles DR, Smail MA, Negus IS, et al. Comparison of radiation doses from multislice computed tomography coronary angiography and conventional diagnostic angiography. *J Am Coll Cardiol*. 2006;47:1840–1845.
13. Urban BA, Fishman EK. Tailored helical CT evaluation of acute abdomen. *Radiographics*. 2000;20:725–749.
14. Sun Z, Winder J, Kelly B, et al. Assessment of VIE image quality using helical CT angiography: in vitro phantom study. *Comput Med Imaging Graph*. 2004;28:3–12.

15. Rydberg J, Kopecky KK, Lalka SG, et al. Stent grafting of abdominal aortic aneurysms: pre- and postoperative evaluation with multislice helical CT. *J Comput Assist Tomogr*. 2001;25: 580–586.
16. Armerding MD, Rubin GD, Beaulieu CF, et al. Aortic aneurysmal disease: assessment of stent-graft treatment-CT versus conventional angiography. *Radiology*. 2000;215: 138–146.
17. Verdun FR, Theumann N, Poletto PA, et al. Impact of the introduction of 16-row MDCT on image quality and patient dose: phantom study and multi-centre survey. *Eur Radiol*. 2006;16: 2866–2874.
18. Semmens JB, Lawrence-Brown MM, Hartley DE, et al. Outcomes of fenestrated endografts in the treatment of abdominal aortic aneurysm in Western Australia (1997–2004). *J Endovasc Ther*. 2006;13:320–329.